Available online at www.sciencedirect.com
ScienceDirect
Atmospheric Environment 42 (2008) 87–100
ATMOSPHERIC ENVIRONMENT
www.elsevier.com/locate/atmosenv

Modeling assessment of point source NO_x emission reductions on ozone air quality in the eastern United States

J.M. Godowitch[a,*,1], A.B. Gilliland[a], R.R. Draxler[b], S.T. Rao[a]

[a] *Air Resources Laboratory, Atmospheric Sciences Modeling Division, National Oceanic and Atmospheric Administration, Research Triangle Park, NC 27711, USA*

[b] *Air Resources Laboratory, National Oceanic and Atmospheric Administration, Silver Spring, MD 20910, USA*

Received 12 February 2007; received in revised form 7 September 2007; accepted 7 September 2007

Abstract

This study investigates the effects of reductions in nitrogen oxide (NO_x) emissions from major point sources on daily maximum 8-h ozone concentrations in the eastern United States. The Community Multiscale Air Quality (CMAQ) model was utilized in photochemical simulations on a matrix of modeling scenarios permitting an examination of the separate effects of emission changes and meteorological influences on maximum ozone levels over a 3-month period during the summers of 2002 and 2004. Two modeling scenarios involved base case 2002 emissions and post-control emissions, reflecting the point source NO_x emission reductions implemented before the ozone season of 2004, using summer 2002 meteorological conditions. Results revealed that point source NO_x emission reductions caused decreases in daily maximum 8-h ozone concentrations over the eastern United States. At the 50th and 95th percentiles of the cumulative frequency distribution, daily maximum 8-h ozone values in the emission reduction scenario were lower than corresponding base case values over 70% and 90% of the modeling domain, respectively. During southwesterly wind flows across the Ohio River Valley, morning ozone concentrations aloft were lower over northeastern states downwind of the emissions-rich region in the NO_x reduction scenario results. Another notable feature of the NO_x emission reduction scenario results is that greater decreases in daily maximum 8-h ozone occurred at higher concentrations. Results from other modeling scenarios revealed strong differences in meteorological conditions between these two summer periods greatly impacted the daily 8-h maximum ozone concentrations with the meteorological effects on ozone being greater than those from emission changes over the northern part of the modeling domain. Using backtrajectory analysis, greater percentage decreases in daily maximum 8-h ozone occurred at monitoring sites when they were downwind of the Ohio River Valley, which is a notable emission source region, as compared to cases when the sites were not downwind of it.
Published by Elsevier Ltd.

Keywords: Photochemical ozone; NO_x emission reductions; CMAQ; HYSPLIT; Trajectory analysis

1. Introduction

Numerous emission control programs have been implemented by the US Environmental Protection Agency (EPA, 2005) in a concerted effort to reduce ground-level ozone concentrations by reducing

*Corresponding author. Tel.: +1 919 541 4802; fax: +1 919 541 1379.
E-mail address: James.Godowitch@noaa.gov (J.M. Godowitch).

[1] In partnership with the US Environmental Protection Agency.

1352-2310/$ - see front matter Published by Elsevier Ltd.
doi:10.1016/j.atmosenv.2007.09.032

emissions of volatile organic compounds (VOCs) or nitrogen oxides (NO_x), the key precursor species involved in the photochemical production of ozone (O_3), in various source categories. Although there has been a downward trend in ozone levels, daily maximum 8-h O_3 concentrations have continued to exceed acceptable limits in widespread areas of the eastern United States. Findings of the OTAG (Ozone Transport and Assessment Group, 1997) program revealed that interstate transport of O_3 and its precursors contributed to elevated ozone concentrations in the northeastern United States. Consequently, EPA issued an emission control policy known as the NO_x State Implementation Plan (SIP) Call. The NO_x SIP Call rule was designed to reduce the interstate transport of ozone and its precursor species by requiring substantial NO_x emission reductions from point sources in 22 eastern states with full implementation of controls to be completed by the summer 2004 ozone season (EPA, 2005).

It is important to assess whether a major emission reduction program achieves particular objectives and provides an improvement in ambient air quality. This task has been challenging since both emissions and meteorological conditions have important roles in ozone formation and accumulation. In particular, variability in key meteorological factors (i.e. temperatures and moisture parameters) can be considerable in different ozone seasons, which complicates any assessment of multi-year ozone changes solely to an emissions change signal. However, advances have occurred in observation-based analysis methods (e.g. Gego et al., 2007) and modeling strategies (e.g. Kim et al., 2006) to take advantage of available measurements in efforts to discern the separate impacts from concurrent meteorological and emissions signals on ozone changes over multiple summer seasons.

The grid-based modeling approach applied in this effort involves photochemical simulations with the Community Multiscale Air Quality (CMAQ) model to investigate the effectiveness of this NO_x emission reduction program in decreasing ambient ozone concentrations. In order to perform a credible assessment of air quality change, accurate point source NO_x emission measurements are vital and the emissions change must be sufficient to cause a detectable improvement in concentrations over a region. Consequently, the routine emissions data from Continuous Emissions Monitoring Systems (CEMS) at major point sources were used in the model simulations. An examination by Frost et al. (2006) indicated the high reliability of the CEMS emission data and reported that notable NO_x emission reductions had already occurred at numerous major point sources by the third quarter of 2003 across the eastern US Frost et al. (2006) also presented initial results from a coupled meteorological–chemical model with a 27 km grid spacing from a selected day during summer 2004 to highlight the varied ozone response due to different emission rates and location of major NO_x point sources. Kim et al. (2006) conducted an extensive examination of the effects of point source emissions reductions due to the NO_x SIP Call and found strong agreement between modeled and satellite-based nitrogen dioxide (NO_2) vertical column values on a regional scale by modeling the entire summer 2004 season. They also reported decreases in vertically averaged ozone due to the NO_x emission reductions. Our CMAQ model simulations, using a finer grid resolution, spanned an entire 3-month period during both summers of 2002 and 2004 which corresponded to ozone seasons before and after implementation of the NO_x emission controls, respectively. Modeling a continuous period over a season is believed to provide a more reliable assessment of the efficacy of an emissions control strategy (Hogrefe et al., 2000).

An examination of the model response to the point source NO_x emission changes is emphasized herein, however, an evaluation of the base case simulation results from both summer periods is also reported to illustrate model performance in estimating daily maximum 8-h ozone concentrations. Recent model evaluations of CMAQ (Appel et al., 2007; Eder and Yu, 2006) have also demonstrated its capability of estimating ozone and other species concentrations. It is acknowledged that changes in another key NO_x emission sector (e.g. mobile) also occurred from 2002 to 2004 (EPA, 2005), which are not considered in this modeling study, since our objective was to focus on the impact of point source emission changes due to the NO_x SIP Call program. Separate model simulation results, which contain the full array of emission changes, are described in a dynamic evaluation of CMAQ (Gilliland et al., 2007) where the model's ozone response is compared to observational results of ozone change. Results from the modeling scenarios herein focus on ground-level daily maximum 8-h ozone, since it is important from a regulatory perspective. Nevertheless, since the NO_x emissions from the major

point sources are continuous elevated releases, the effect on modeled concentrations aloft is also briefly explored to assess overnight transport of ozone and its precursors in the residual layer. Furthermore, modeling results based on trajectory analysis are presented to examine the impact on maximum ozone levels from NO_x emission reductions when specific sites are situated downwind and not downwind of a major point source emission region.

2. Data sets and modeling methods

2.1. Observational data sets

The ozone measurements used in this study were collected at monitoring sites of the Clean Air Status and Trends Network (CASTNet; http://www.epa.gov/castnet) which are situated in primarily rural locations of the United States and are relatively distant from notable local sources. The hourly ozone data at 56 monitoring sites in the eastern US were processed in order to determine daily maximum 8-h O_3 concentrations over the 3-month modeling periods for use in the model evaluation and modeling analysis.

Major US point sources, primarily electrical generating units at fossil-fuel power plants and large industrial sources, are equipped with CEMS in order to acquire hourly measurements of NO_x and SO_2 emissions (http://www.epa.gov/airmarkets/emissions). The hourly CEMS data for the summer seasons of 2002 and 2004 were analyzed and also included in the model simulations.

2.2. Model description and modeling scenarios

The CMAQ modeling system (version 4.5) was applied in this study. CMAQ is a comprehensive Eulerian air quality grid model designed for assessments of multiple atmospheric pollutants, including O_3 and other oxidants, aerosols, air toxic and mercury species on urban to continental scale domains. CMAQ is composed of state-of-science algorithms designed to solve the relevant dynamic, chemical, and atmospheric removal processes. For the photochemical simulations performed in this study, the CB4 gas-phase chemical mechanism with updates described by Byun and Schere (2006) was employed in conjunction with the computationally efficient Euler backward iterative (EBI) chemistry solver. The model was configured to include horizontal and vertical advection, turbulent diffusion in the horizontal and vertical based on K-theory, gaseous and aqueous phase chemistry, cloud effects on photolysis rates, and dry and wet deposition processes. The theoretical formulations and numerical algorithms used to treat these physical and chemical processes in CMAQ are described in Byun and Schere (2006).

Meteorological fields were generated by the Penn State/NCAR fifth-generation mesoscale model (MM5; Grell et al., 1994). The MM5 model (version 3.6.3) was applied in a non-hydrostatic mode and included a four-dimensional data assimilation technique to incorporate observed wind, temperature, and moisture data to provide more accurate three-dimensional modeled fields. Additionally, the land-surface scheme by Xiu and Pleim (2001) was used to improve model response to varying soil moisture and vegetation conditions over the summer season. The CMAQ Meteorology–Chemistry Interface Processor (MCIP v3.1) program was exercised to reformat the MM5 output from 30 levels into model-ready input data sets containing the hourly two-dimensional and three-dimensional meteorological parameter fields utilized in the CMAQ model simulations.

The emission data sets were generated by the comprehensive Sparse Matrix Operator Kernel Emissions (SMOKE version 2.2; http://www.smoke-model.org) processing system. Anthropogenic emissions from the EPA 2001 National Emissions Inventory (NEI version 3) were used to generate surface and elevated non-CEMS point source emissions. Natural surface emissions were computed by the Biogenic Emissions Inventory System (BEIS version 3.13). The MOBILE6 model was applied to use projections of vehicle-miles-traveled (VMT) and fleet factors to develop gridded motor vehicle emissions for the 2002 and 2004 periods. The SMOKE point source processor computed plume rise using stack parameters and meteorological fields in order to vertically allocate point source emissions, including CEMS point source emissions, into model layers.

The modeling domain spanned a much broader region than the area of the states involved in the NO_x SIP Call program by encompassing the eastern half of the United States and southeastern Canada. There are 205×199 horizontal grid cells with a 12 km grid cell spacing. The vertical structure contained 14 layers defined on a sigma-pressure, terrain-following coordinate system. The approximate thickness of layer 1 was 38 m and for reasonable resolution within

the daytime mixing layer, the mid-layer heights of the first eight model layers were at about 19, 115, 230, 385, 585, 915, 1380, and 1918 m a.g.l. with the top layer extending to 15.3 km a.g.l.. Initial conditions and lateral boundary concentrations for each modeling scenario were specified with the same set of time-invariant, vertically varying tropospheric background estimates. Specifically, ozone along the lateral boundaries was defined to be 35 ppb in layer 1 and it was incrementally increased layer-by-layer to 48 ppb in layer 9 and 70 ppb in layer 14. The modeling period was from 1 June through 31 August in 2002 and 2004, and there was a 10-day model spin-up period before 1 June.

Table 1 identifies the set of modeling scenarios designed to permit an investigation of the separate impacts on O_3 concentrations due to emission changes and from differences in meteorological conditions. Comparisons of the M02E02 and M04E04 scenario results, described in Gilliland et al. (2007), illuminate the combined effects of changes in meteorology and emissions on ozone levels between the two summer periods. Differences between the M02E02 and M04E02 modeling scenarios demonstrate the impact of meteorological variations alone on ozone levels. Of particular interest herein, an examination of the base case results (M02E02) with those from the M02E04 modeling scenario provides an assessment of point source NO_x emission changes on ozone levels under summer 2002 meteorological conditions. In order to assess the NO_x emission control effect, the key difference between the E02 and E04 emission data sets in these modeling scenarios was in the use of summer 2004 CEMS data, which reflected the point source NO_x reductions. Emissions in other source categories remained unchanged.

2.3. Trajectory modeling

The HYbrid Single Particle Lagrangian Integrated Trajectory (HYSPLIT, Draxler and Hess, 1997) model was applied to generate backward trajectories originating from each CASTNet site location in order to identify cases when the airflow arriving during the mid-afternoon on each day at a site had previously passed through the Ohio River Valley (ORV) region, since it contained numerous point sources exhibiting large NO_x emission reductions. Backward trajectories were initiated at 1900 UTC starting at 250 m a.g.l. and were tracked for 24, 48, and 72 h upwind from sites whose distances were up to 400 km, 400–800 km, and over 800 km away from the ORV region, respectively. Coordinates of each back trajectory were analyzed to determine if it was located inside the designated region representing the ORV (Fig. 12). For this trajectory analysis, the same three-dimensional wind fields applied in the CMAQ simulations were also used in the HYSPLIT calculations.

Table 1
Matrix of CMAQ model simulation scenarios for different summer periods with different emission data sets

Emissions	Summer meteorology	
	2002	2004
2002	M02E02	M04E02
2004	M02E04	M04E04

3. Results and discussion

3.1. Model evaluation results

Before addressing the model's ozone response from the emission reductions, results of a model performance evaluation are presented to examine CMAQs capability to estimate daily maximum 8-h ozone concentrations. Model results from the base case scenarios for both summer periods (i.e. M02E02 and M04E04) were involved in this evaluation. The modeled maximum 8-h O_3 concentration from the grid cell containing a measurement site was paired with a non-missing observed maximum 8-h O_3 value at each CASTNet site for each day of the simulation periods. The statistical metrics in Table 2, which were utilized and also defined in Eder and Yu (2006), include measures of model bias (i.e. mean bias (MB) and normalized mean bias (NMB)) and measures of model error (i.e. root mean square error (RMSE) and normalized mean error (NME)) as well as the correlation coefficient (r) derived from a linear regression fit to each set of paired values. The summary results in Table 2 reveal that daily maximum 8-h ozone was slightly underestimated ($MB = -2.1$ ppb) during the summer 2002 and overestimated ($MB = +4.0$ ppb) during summer 2004 by the model. The model exhibited less error for the summer 2002 period with a NME of 16.2% versus 17.9% for the summer of 2004, and the relatively high correlation coefficient of 0.81 for summer 2002 is >0.70 obtained from summer 2004 results. These

Table 2
Summary statistical results for maximum 8-h ozone concentration pairs from both summer periods

	N	Obs. (ppb)	Mod. (ppb)	MB (ppb)	RMSE (%)	NMB (%)	NME (%)	*r*
2002	4962	55.9	53.8	−2.1	11.5	−3.8	16.2	0.81
2004	4915	45.0	49.0	4.0	10.2	8.9	17.9	0.70

Note: Obs., observed mean, Mod., modeled mean, r = correlation coefficient from linear regression fit, and N, number of concentration pairs.

statistical results are quite similar to those obtained with this version of the CMAQ model for the summer 2001 ozone season (Appel et al., 2007).

Since summary statistics give a partial picture of overall model performance, additional analyses of modeled and observed maximum 8-h O_3 were also undertaken to examine aspects of CMAQs treatment of the spatial variability and temporal behavior of maximum 8-h ozone levels during the warmer, drier summer 2002 period. Modeled and observed daily maximum 8-h concentration pairs averaged over the entire modeling period for each site are displayed in Fig. 1a. These results reveal that CMAQ tended to overestimate maximum 8-h ozone in the lower concentration range at most sites situated around the perimeter of the modeling domain, except for two mid-western sites close to the western boundary. In contrast, model results underestimated maximum 8-h ozone values at higher concentration levels occurring at CASTNet sites within the interior of the domain which are found in the southeast and ORV regions, and the mid-Atlantic and northeastern states (Fig. 12). Boundary conditions are believed to have a role in affecting these evaluation results, particularly at the sites closer to the boundaries. Temporally and spatially varying boundary concentrations prescribed from continental-scale or global model results might have improved the results somewhat for both sets of sites.

The time series of domain-wide, daily maximum 8-h O_3 values determined from modeled and observed concentrations from all sites are displayed in Fig. 1b over the entire summer 2002 period. The day-to-day variations in the CMAQ results replicate the observed daily variations quite well, which indicate the model accurately captured the build-up and departure of the regional ozone concentration pattern associated with synoptic-scale air mass movement and frontal propagation across the region during this summer season. However, during multi-day events exhibiting elevated ozone levels and two notable high ozone episodes (i.e. 18–25 June and 10–14 August) evident in Fig. 1b, CMAQ tended to underestimate maximum 8-h ozone levels with greater negative average biases, while overestimating observed values at lower ozone levels

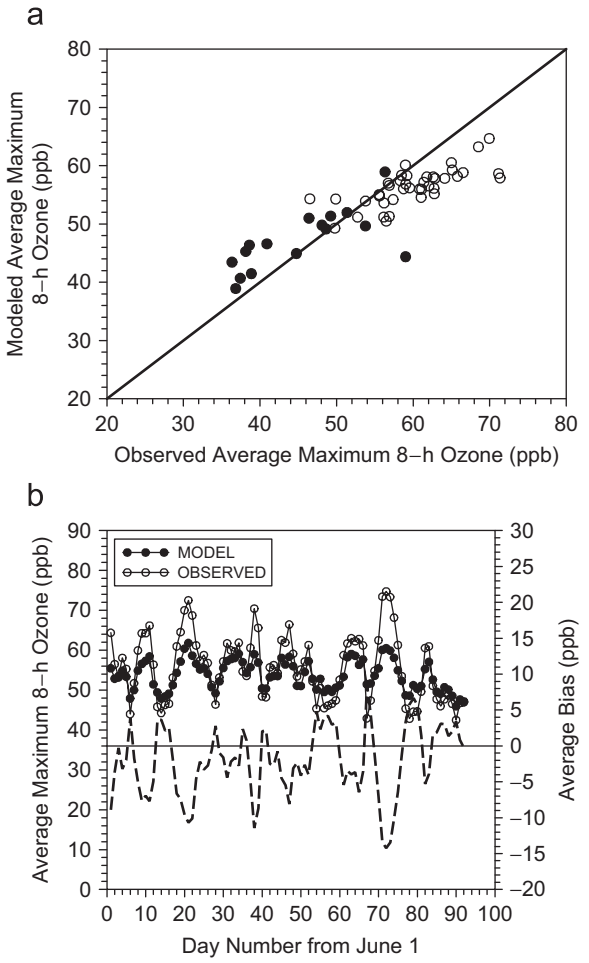

Fig. 1. (a) Comparison of observed and modeled average maximum 8-h ozone at each CASTNet site over the summer 2002 period. Sites along the periphery of the modeling domain and in the interior are denoted by solid and open circles, respectively, and (b) daily observed (○) and modeled (●) maximum 8-h ozone averaged over all sites on each day of summer 2002 and daily average model bias (---).

associated with cloudy, wet periods. Nevertheless, the average bias was found to be within ±5 ppb on about 90% of these summer days. In a comparative study of chemical mechanisms, Arnold and Dennis (2006) noted that CB4 chemistry generally produced less O_3 than other chemical mechanisms. However, of greater relevance, the relative (percentage) O_3 response with CB4 to NO_x emissions change is similar to the SAPRC99 chemical mechanism under similar meteorological conditions (Gilliland et al., 2007). Results on most days during summer 2004 (not shown) substantiated the overall positive bias exhibited in the evaluation results for the summer 2004, which was characterized by abnormally cool, wet conditions across the mid-western states and most of the eastern US (White et al., 2006). In fact, the mean daily observed maximum 8-h O_3 value for summer 2004 is nearly 11 ppb lower relative to summer 2002 in Table 2, which reflects the effects of changes in both emissions and meteorological conditions.

3.2. Point source NO_x emission changes

The locations of the largest point sources with CEMS measurements in the modeling domain and the percentage change in their NO_x emissions due to the NO_x SIP Call program are depicted in Fig. 2 from a typical summer case. Although 987 grid cells contained a CEMS point source, each NO_x point source displayed in Fig. 2 emitted at least 20 t day^{-1}. Substantial reductions in NO_x emissions of >80% are evident at several individual sources in Fig. 2, particularly at the largest NO_x-emitting point sources located within the ORV region. Although notable NO_x emission reductions are also apparent at some point sources found outside the ORV, most of these sources are relatively isolated and are not in as close proximity to each other as those situated within the ORV region.

Since these major point source emissions are released from tall stacks into plumes which generally exhibit considerable buoyancy, it is of interest to examine the plume heights of these high NO_x emissions within the model's vertical structure. Fig. 3 displays vertical profiles of NO_x emissions for the base and emission reduction scenarios from the point sources within the central/upper ORV region in Fig. 2, and from point sources located outside the ORV for a typical summer case. The NO_x emission contributions from all point sources found within each model layer were summed and

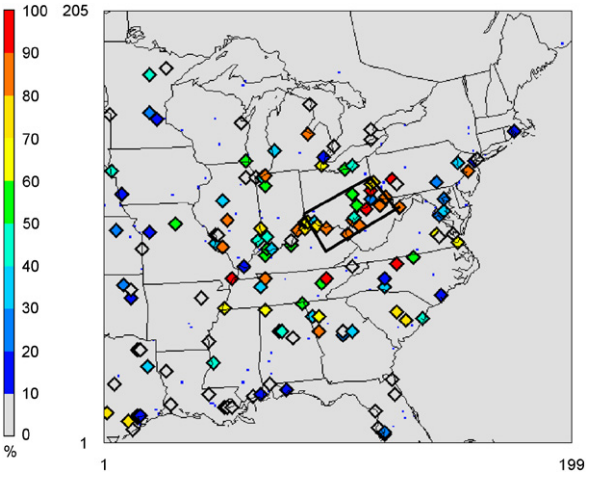

Fig. 2. Reduction (%) in NO_x emissions at major point sources in the modeling domain between the base and post-control scenarios for a typical summer case (26 June, 2002). The Ohio River Valley sources are denoted inside the box.

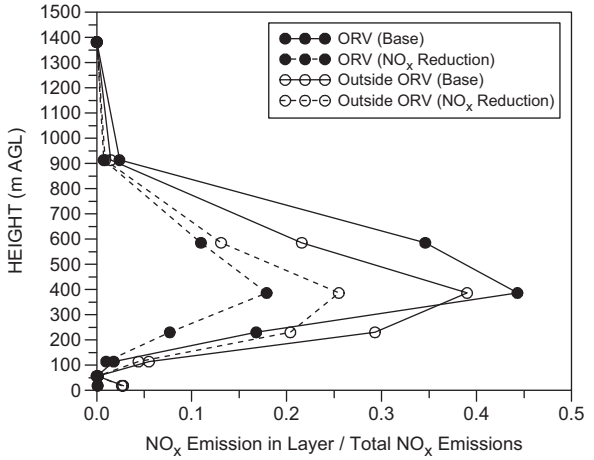

Fig. 3. Vertical distribution of point source NO_x emissions at model mid-layer heights from CEMS sources inside and outside the Ohio River Valley (ORV) region from the base and reduction scenarios for a typical summer case (26 June, 2002). Values are normalized by the base emission totals of 2.77 and 8.93 kt day^{-1} for CEMS sources inside and outside the ORV, respectively.

then normalized by the daily total NO_x emissions in each group in order to determine the fractional amount of emissions released into each vertical layer. The total NO_x emissions from CEMS point sources were 11.7 kt with the ORV sources emitting 2.77 kt of the total in this case. Fig. 3 indicates most CEMS point source emissions are released at heights ranging from 200 m to about 600 m. At these heights, considerable transport of elevated NO_x concentrations in plumes is possible due to

higher winds aloft, particularly during the nocturnal period. While a notable decrease in NO_x emissions is evident between the base and the emission reduction scenarios in both groups, the point source emissions in the ORV region display a much greater percentage emission reduction than those outside the ORV. In fact, the highest NO_x emissions near 400 m within the ORV in the base case were reduced by over 60% after controls compared to just 33% for the group outside the ORV at this level. Thus, a significant decrease in available NO_x for horizontal transport aloft occurred after implementation of the emission controls at point sources within the relatively confined area of the ORV.

The difference in the total CEMS measurements over the 3-month period revealed a 36.4% drop in NO_x emissions in this major point source sector from 1022 to 651 kt between the summer 2002 and 2004 periods, respectively. The hourly emissions also exhibited a similar decrease over all hours of the diurnal cycle. As noted earlier, mobile NO_x emission changes, which were estimated to decrease by about 11.5% between the two seasons, are not considered in these modeling scenarios. However, the mobile source sector contribution remained at about 38% of the total NO_x emissions budget in this domain. The total NO_x emissions from all source categories in the modeling domain were 4267 and 3896 kt over the summer 2002 and 2004 simulation periods, respectively. Therefore, putting this point source NO_x emission change into perspective when considered within the total NO_x emission budget, the NO_x emission reduction in the CEMS sector dropped its contribution from 24% to 16.7% of the total domain-wide NO_x emissions between the M02E02 and M02E04 modeling scenarios. Finally, the decrease in total NO_x emissions in the modeling domain due to the CEMS point source NO_x reductions was 8.7%.

3.3. Impacts on daily maximum 8-h ozone concentrations

The daily maximum 8-h ozone concentration on each simulation day was computed for each grid cell for these modeling scenarios and the cumulative frequency distribution of maximum 8-h O_3 values for each grid cell was also determined. The gridded fields of daily maximum 8-h O_3 at the 95th percentile are displayed in Fig. 4 to show the spatial pattern and magnitude of this high ozone level from the base case results for the summer 2002 (M02E02) and summer 2004 (M04E04) modeling scenarios. The results for the summer 2002 are more common of a typical summer ozone season with higher ozone occurring in the mid-Atlantic and northeastern urban corridor, the greater ORV region and mid-western states, as well as near notable urban areas of the southeastern states. The modeled maximum ozone values during the summer 2004 were considerably lower relative to summer 2002. Frequent cold fronts associated with numerous low-pressure

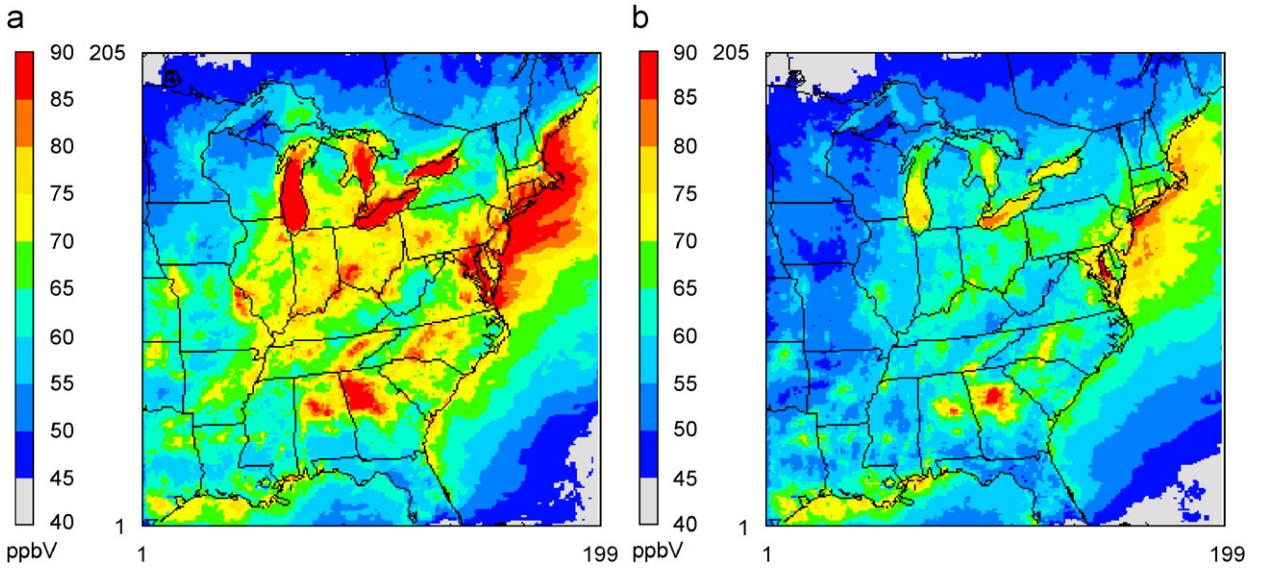

Fig. 4. Maximum 8-h O_3 concentration fields at the 95th percentile from base case results from the (a) summer 2002 (M02E02) scenario and (b) summer 2004 (M04E04) scenario.

areas which developed and traveled through the region were followed by cool air masses moving into the eastern states. Consequently, weather conditions during the summer of 2004 were not conducive to significant ozone formation and relatively few ozone exceedances occurred in the northeastern states compared to the summer 2002 (White et al., 2006).

3.3.1. Meteorological effects on ozone levels

The impact of differences in meteorology between these two summer periods is further explored with the results of the M02E02 and M04E02 modeling scenarios, which were performed with different meteorological data sets and the same emissions. Fig. 5 depicts the average percent difference field in daily maximum 8-h O_3 due to the meteorological effects. These results represent the average percentage change computed from the differences over individual percentiles between the 5th and 95th percentiles of the cumulative distributions of maximum 8-h ozone values for each modeling scenario. Noticeably lower daily maximum 8-h O_3 over most of the domain during the summer 2004 period is attributed to the unfavorable meteorological conditions. The largest percentage impacts in Fig. 5 are exhibited across the mid-western states with values 12–16% lower during 2004, while decreases in maximum 8-h ozone of approximately 10% occurred within the ORV region. The difference field in the mean modeled maximum temperature between the summer periods displayed in Fig. 6 reveals the expected close correspondence between areas exhibiting relatively cooler maximum temperatures and those areas with the largest percentage decreases in maximum 8-h O_3 in Fig. 5. The average maximum temperatures were substantially cooler by as much as 3–5 °C during the summer 2004. Results obtained from the M02E04 and M04E04 scenarios also reinforced these same findings. Hence, meteorological effects on modeled maximum ozone levels were indeed substantial between these two summer periods and demonstrate the need to account for meteorological effects when assessing differences in O_3 levels across different summer seasons in order to properly discern the signal due to concurrent emission changes.

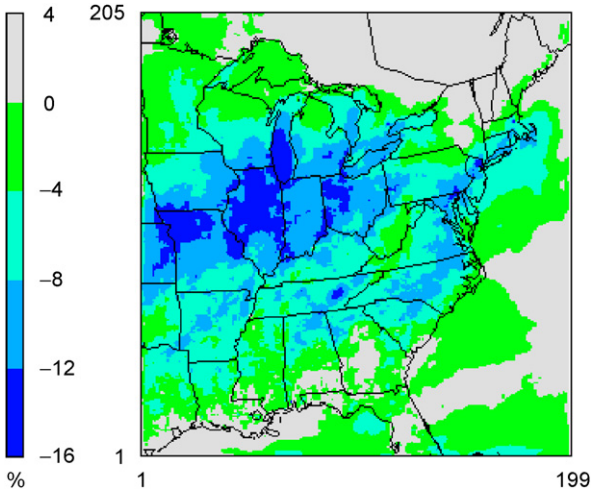

Fig. 5. Impact (% change) on the daily maximum 8-h O_3 due to differences in meteorological conditions between the M02E02 and M04E02 modeling scenarios. Results represent the gridded average computed from the individual differences over the 5–95th percentiles of the cumulative concentration distributions.

3.3.2. Emission effects on maximum ozone levels

The effect of the point source NO_x emission reductions alone (i.e. M02E02 versus M02E04 scenarios) on maximum 8-h ozone is revealed in Fig. 7, which depicts the spatial difference fields at the 50th and 95th percentiles of the cumulative frequency distributions of maximum 8-h ozone values. Both results indicate sizeable areas of the domain experienced decreases in maximum 8-h O_3 in the NO_x reduction scenario. However, the area of the domain exhibiting lower maximum O_3 values at the 95th percentile is 90% compared to 70% at the 50th percentile. In addition, the areas with a maximum ozone reduction exceeding 2.5% are 9.6% and 31% of the domain at the 50th and 95th percentiles, respectively. It is apparent the

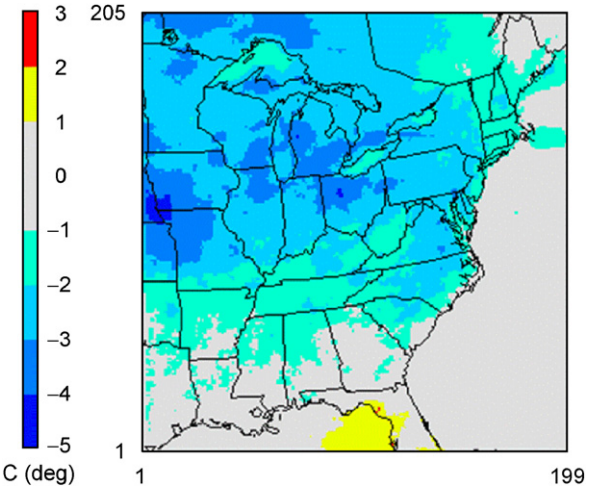

Fig. 6. Average difference (2004–2002) in modeled 3-month mean maximum temperatures between the summer periods.

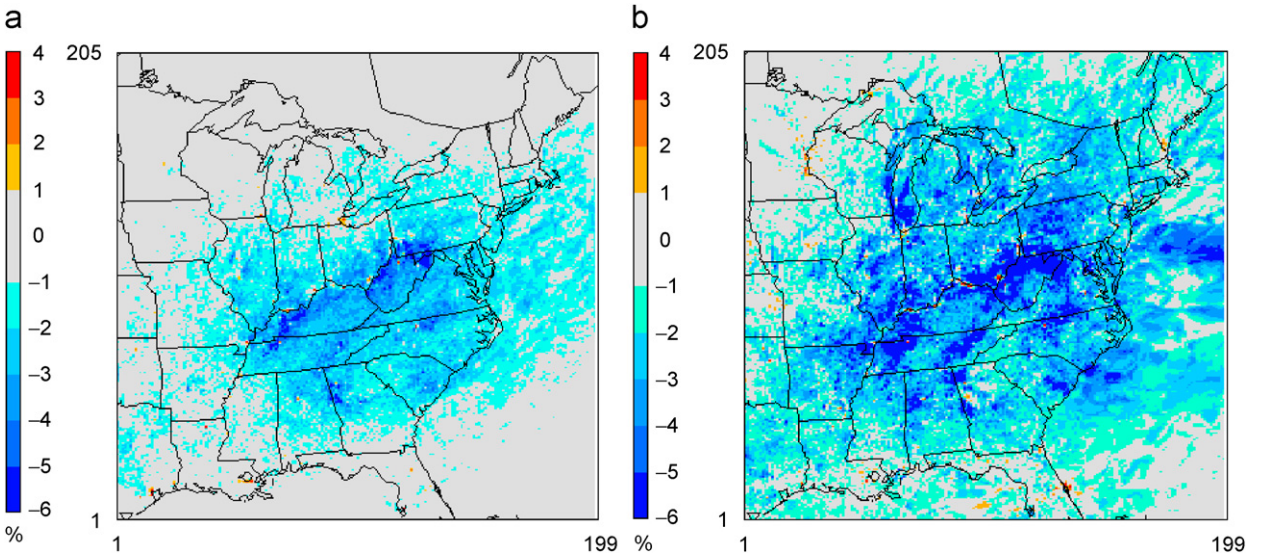

Fig. 7. Percent difference results [(M02E04−M02E02) × 100/M02E02] in the daily maximum 8-h O_3 concentrations at the (a) 50th percentile and (b) 95th percentile. Note the same scales in both figures.

ozone reductions at the 95th percentile level were greater. At the 50th percentile, the largest decrease was 8% which was found close to major point source grid locations in the ORV, while the maximum O_3 reduction at the 95th percentile was as high as 18% in comparable locations. These results indicate that the impact of the emissions changes was greater at higher ozone concentrations. Probability density distributions (not shown) of the modeled maximum 8-h ozone values also indicated a detectable shift away from higher concentrations with increases in the frequencies at lower concentration levels in the NO_x emission reduction scenario results.

It is also of interest to compare these results with those from the M04E02 and M04E04 modeling scenarios which employed the unfavorable meteorological conditions for ozone formation during summer 2004. Interestingly, results from these scenarios were found to be quite comparable to those in Fig. 7 even at the lower maximum 8-h ozone levels experienced during the summer 2004. The fractional area of the domain exhibiting ozone reductions was also nearly the same as the summer 2002 results noted above. The largest relative decreases in maximum O_3 at the 50th and 95th percentiles are 9% and 13% for the summer 2004 scenario results, the latter being somewhat lower than the value obtained from the summer 2002 results. Furthermore, these results are in agreement with the spatial O_3 difference pattern in Kim et al. (2006) from different emission modeling scenarios for the summer 2004 period. They reported the largest decrease in vertically averaged O_3 (i.e. 7 ppb decrease out of a 72 ppb average base value) was within the ORV region and also noted the emission reduction effects diminished considerably at long distances from the source regions.

With a 3-month modeling period, a variety of weather conditions and flow patterns were simulated and more cases for similar flow regimes were also obtained. The daily synoptic weather maps, modeled wind flows across the ORV region, and modeled ozone difference patterns were examined to classify the summer 2002 days into four distinctive groups exhibiting different flow patterns in order to assess the impact on maximum ozone for each synoptic regime. Fig. 8 depicts the average percentage difference fields in maximum 8-h ozone levels between the M02E02 and M02E04 results under southwesterly (SW, 19 cases), predominately westerly (W, 17 cases), northerly (N, 18 cases), and generally south/southerly (S/SE, 14 cases) flow regimes. Days with a front or low-pressure area in the ORV region were omitted. Results in Fig. 8 illustrate the strong influence of transport during these various synoptic flow patterns on the downwind area impacted by decreases in maximum 8-h ozone due to the NO_x point source emissions reductions. In particular, Fig. 8a for the SW flow

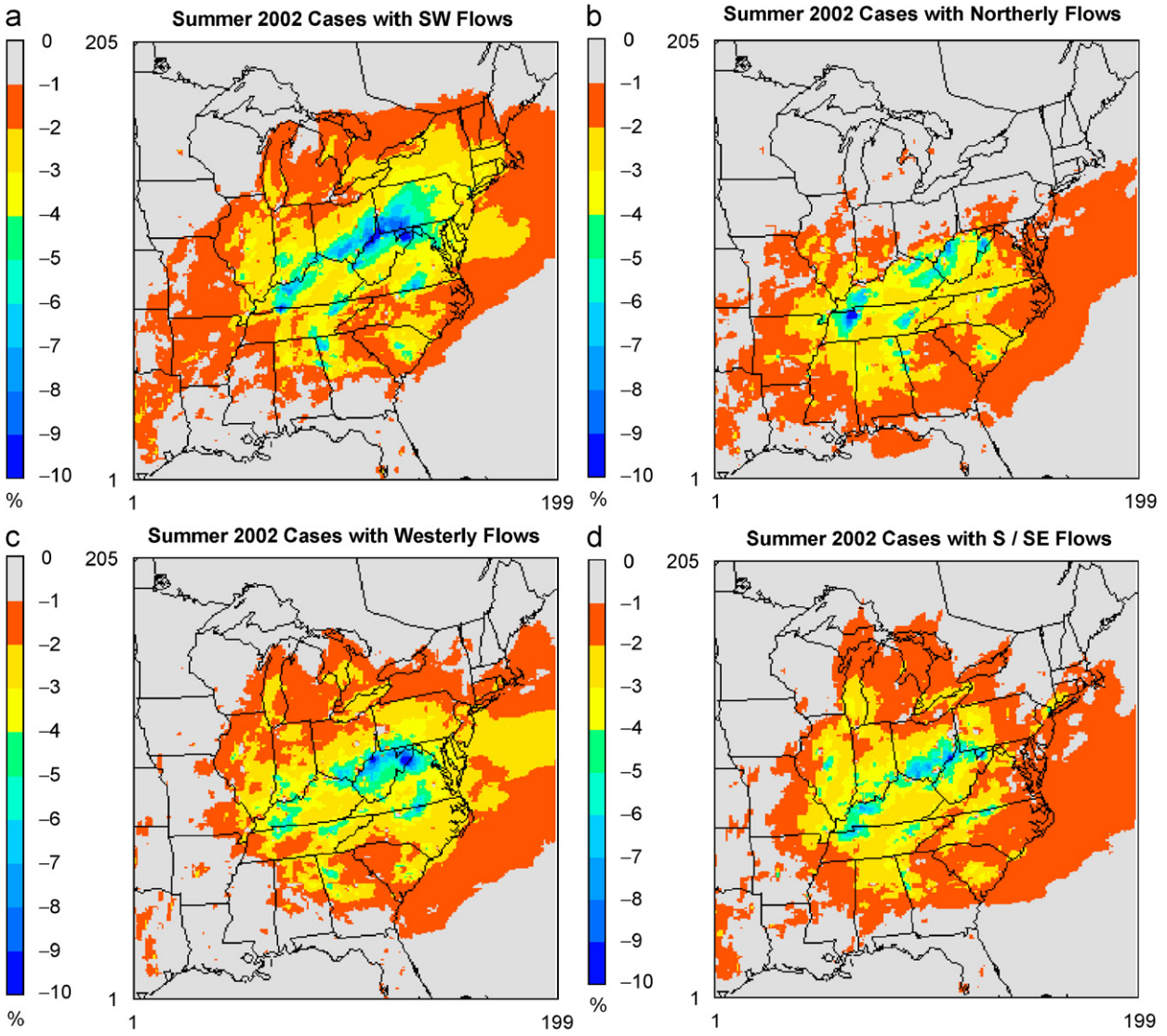

Fig. 8. Average percent reduction in daily maximum 8-h O_3 for different flow regimes during summer 2002: (a) southwest (SW), (b) northerly (N), (c) westerly (W), and (d) south-southeasterly (S/SE) wind flow patterns.

cases shows a more pronounced area of greater ozone reduction extending downwind of the ORV toward the northeastern US that is not as evident in the downwind areas under the other flow regimes. This result is attributed to the close alignment of the major point sources in the ORV with the SW wind flow pattern and enhanced the benefits of the NO_x reductions farther downwind. Nevertheless, noticeable decreases in maximum O_3 are also exhibited in areas downwind of the ORV due to the NO_x emission reductions under the other flow patterns, which is explored further in the trajectory analysis. The S/SE cases experienced the slowest wind flows, so the notable decreases in maximum 8-h O_3 in Fig. 8d are primarily confined closer to the ORV region.

3.3.3. *Concentration changes aloft*

The change in concentrations aloft due to the NO_x emission reductions was explored, and the focus of this analysis is on the SW flow cases during 2002. The NO_x concentrations were examined from model layers 4–6 where the significant NO_x emission reductions occurred (Fig. 3). Fig. 9 displays the average percent difference in NO_x concentrations between M02E02 and M02E04 results at a

mid-morning hour (14:00 UTC). Near this time downward vertical mixing of pollutants transported during the nocturnal period often occurs as the daytime convective boundary layer grows to these heights. As expected, Fig. 9 reveals large NO_x concentration decreases of up to 80% near the point sources exhibiting the greatest emission reductions (Fig. 2). However, NO_x concentrations decreases of at least 10% extend downwind of the ORV into north-central Pennsylvania and western New York state.

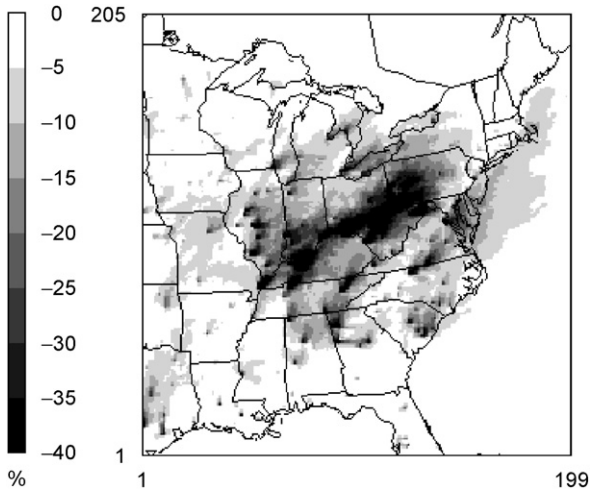

Fig. 9. Average change (%) in modeled NO_x concentrations aloft at 14:00 UTC between the base (M02E02) and NO_x reduction (M02E04) scenarios for SW flow cases.

The SW flow cases consisted of eight sets of two consecutive days exhibiting nearly the same flow pattern. Fig. 10 displays the average percent change in O_3 concentrations aloft (i.e. within layers 4–6) derived from the day 1 set and the day 2 set of consecutive day pairs with SW flows. These model results clearly provide evidence of discernable decreases in O_3 concentrations aloft due to the upwind NO_x emission reductions. Fig. 10b reveals that an interesting spatial displacement occurs from the day 1 to day 2 results as the downwind area exhibiting decreased O_3 shifts further toward the east coast. This feature is attributable to the additional horizontal transport occurring during the second day for these pairs of cases. The decrease in ozone is about 3–5% and is a desirable effect as reduced O_3 aloft will contribute to lower surface O_3 concentrations after being mixed downward during the morning period (Zhang and Rao, 1999). Fig. 10 also shows that O_3 concentrations aloft increase somewhat in point source emission areas. This feature is attributable to less O_3 titration (i.e. removal of O_3 by reaction with NO) due to dramatically lower NO concentrations associated with the substantial point source emission reduction at these heights.

The impact of lower O_3 aloft on surface concentrations is also illustrated by the example

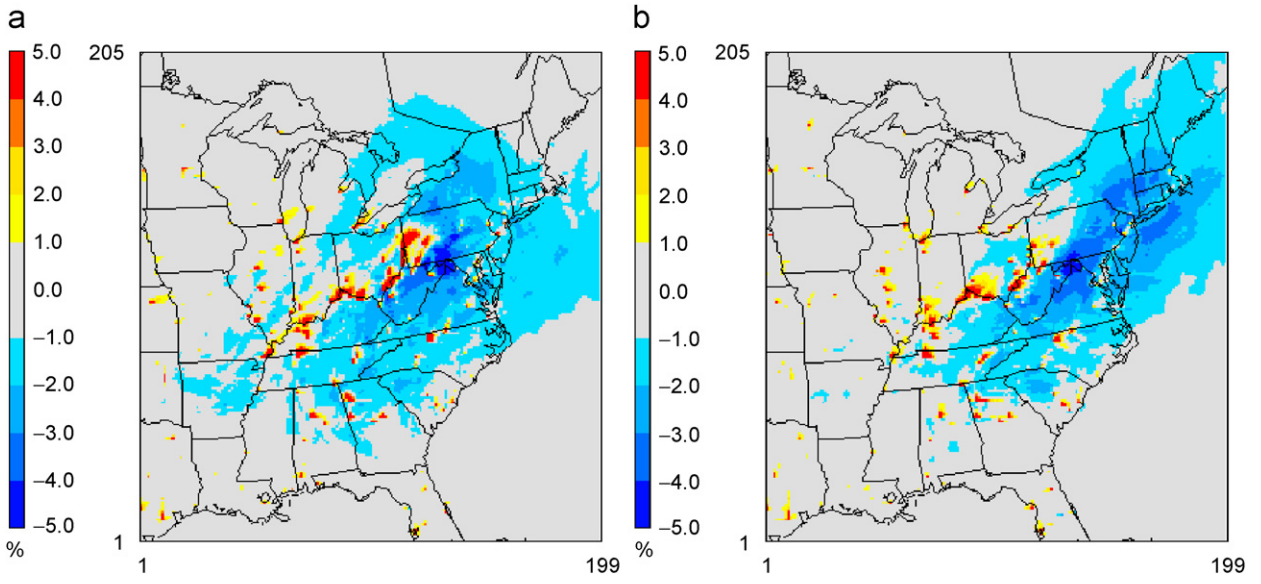

Fig. 10. Average change (%) in ozone concentrations aloft at 14:00 UTC between the NO_x reduction and base (M02E04−M02E02) scenarios for the (a) set of day 1 and (b) set of day 2 cases of SW flow consecutive day pairs.

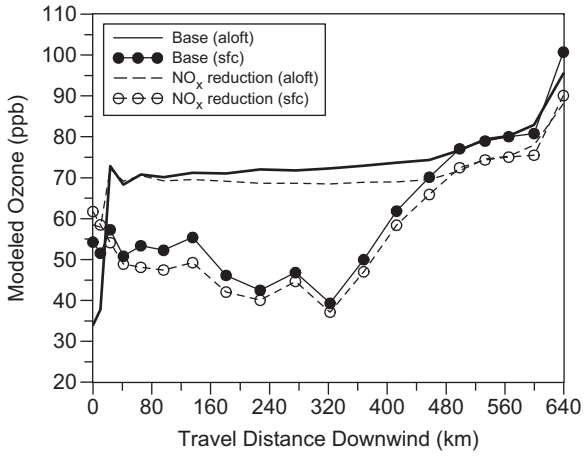

Fig. 11. Modeled O_3 concentrations from the M02E02 and M02E04 scenario results along a forward trajectory path aloft and below in layer 1 starting from the release height of a NO_x point source plume in the ORV region. The trajectory was initiated at 02:00 UTC on June 11, 2002 and the travel duration is 18 h.

case in Fig. 11. Modeled O_3 concentrations aloft and in layer 1 are displayed from the grid cell locations along a forward trajectory path. It was initiated at 02:00 UTC at the emission height of a NO_x point source in the ORV region. Over an 18-h period spanning the nocturnal period and into the next afternoon, the trajectory travels >600 km downwind to the east coast, a result comparable to that reported by Rao et al. (1997). Initially, the O_3 aloft in the base case along the trajectory is relatively low, due to NO titration noted above, but becomes higher further downwind than results from the emission reduction scenario. The near-surface (layer 1) O_3 concentrations below the elevated trajectory path depict the traditional rapid ozone rise during the morning period, which occurs from 320 to 500 km downwind in Fig. 11. During the course of the daytime period, lower surface layer O_3 concentrations are evident in the NO_x reduction scenario results of about 10 ppb at the end of the trajectory in this case. Lower O_3 aloft is primarily attributed to the decrease in afternoon ozone concentration in layer 1 downwind, however, reduced chemical production of O_3 downwind may also be an additional factor which is being investigated from process analysis results from these simulations.

3.3.4. Impact on ozone downwind of a source region

To further examine the impact of the substantial NO_x emission reductions in the ORV region on daily maximum 8-h O_3 values at downwind locations in individual cases, the CASTNet sites were used as starting positions for backward trajectory analyses. Fig. 12 depicts the largest modeled decrease in maximum 8-h O_3 attributed to a direct impact occurring at each CASTNet site location on a particular day in summer 2002. Results indicate larger O_3 reductions closer to the ORV region and at sites which are impacted by other notable point source locations in the domain with NO_x reductions. Backward trajectory analysis using the HYSPLIT model was performed for each site to determine if airflow had earlier passed through the ORV or missed it.

Fig. 13 presents the results composed of modeled percentage decreases paired against the observed maximum 8-h O_3 values from all sites of the summer 2002 period. The modeled percentage decreases in maximum 8-h O_3 were indeed greater from cases when monitoring sites were downwind of the ORV than when they were not downwind of it, consistent with results in Gego et al. (2007). This result is anticipated due to the greater NO_x emission reductions in the ORV sources than for those outside the ORV (Fig. 3). Furthermore, these results also corroborate earlier results showing a trend toward larger relative decreases at higher concentration levels of daily maximum 8-h O_3. A similar finding was reported by Solberg et al. (2005) who determined maximum ozone values decreased at

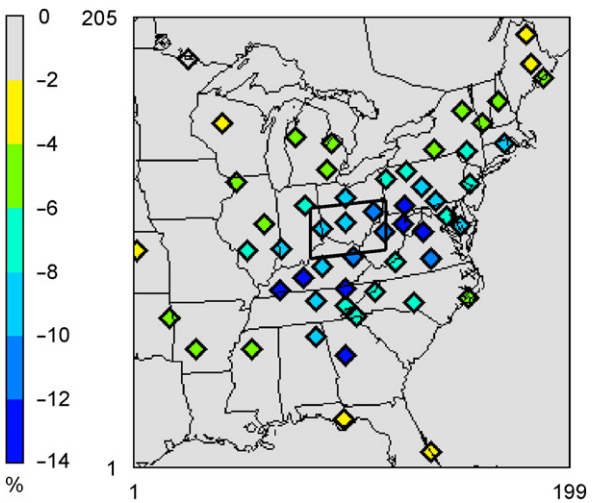

Fig. 12. Largest decrease (%) in maximum 8-h O_3 obtained at the grid cell locations of CASTNet sites between the NO_x reduction and base case (M02E04−M02E02) scenarios. The box shown represents the greater Ohio River Valley (ORV) area used in the trajectory analysis.

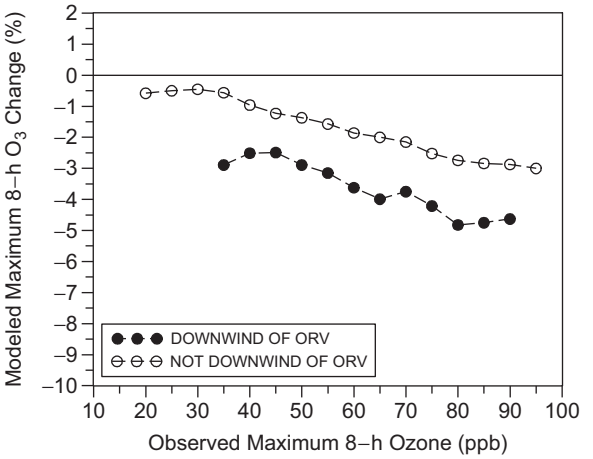

Fig. 13. Percent reduction in daily maximum 8-h O_3 as a function of the observed daily maximum 8-h ozone values at CASTNet sites for downwind cases (solid circles) and not downwind cases (open circles) of the ORV region.

various Scandinavian sites downwind of Western European countries after emission reductions. The relationship displayed in Fig. 13 is a composite over all sites with results at individual sites displaying somewhat different slopes, however, the same general trend was found.

4. Summary

Results of modeling scenarios using base case and point source NO_x emission reductions with the meteorological fields from two different summer periods revealed discernable decreases in daily maximum 8-h O_3 over large areas, especially downwind of the ORV region, which had dramatic NO_x emission reductions due to the NO_x SIP Call program. Model results showed that point source NO_x emission reductions caused significant decreases in NO_x concentrations aloft and evidence of lower ozone concentrations in the residual layer aloft in downwind areas of the eastern US under southwesterly flow cases. Another interesting finding was that greater decreases in maximum ozone values tended to occur at higher concentrations. Trajectory analysis results showed that sites downwind of the ORV region experienced greater decreases in maximum 8-h O_3 than when not downwind of it. Model results indicated that large differences in meteorological conditions between summer 2002 and 2004 also contributed to notable maximum ozone decreases, which exceeded those from the emissions change effect in some areas. These results should be considered specific to this model configuration which applied CB4 chemistry, a 12-km grid resolution and the vertical layer structure used in this study. Time-varying boundary conditions generated from a recent CMAQ simulation on a continental domain should provide improved lateral concentrations for this regional domain and results of additional model simulations involving the total NO_x emission change, including mobile emissions differences, provide a valuable comparison to observed O_3 change (Gilliland et al., 2007).

Dislaimer

The research presented here was performed under the Memorandum of Understanding between the US Environmental Protection Agency (EPA) and the US Department of Commerce's National Oceanic and Atmospheric Administration (NOAA) and under the agreement number DW13921548. This work constitutes a contribution to the NOAA Air Quality Program. Although it has been reviewed by EPA and NOAA and approved for publication, it does not necessarily reflect their policies or views.

References

Appel, K.W., Gilliland, A.B., Sarwar, G., Gilliam, R., 2007. Evaluation of the Community Multiscale Air Quality (CMAQ) model version 4.5: sensitivities impacting model performance, part I—ozone. Atmospheric Environment, in press.

Arnold, J.R., Dennis, R.L., 2006. Testing CMAQ chemistry sensitivities in base case and emissions control runs at SEARCH and SOS99 surface sites in the southeastern U.S. Atmospheric Environment 40, 5029–5040.

Byun, D., Schere, K.L., 2006. Review of the governing equations, computational algorithms, and other components of the Models-3 Community Multiscale Air Quality (CMAQ) modeling system. Applied Mechanics Reviews 59, 51–77.

Draxler, R.R., Hess, G.D., 1997. Description of the HYSPLIT_4 modeling system. NOAA Technical Memorandum Report, ERL, ARL-224, available at: 〈http://www.arl.noaa.gov/ready/hysplit4.html〉.

Eder, B., Yu, S., 2006. A performance evaluation of the 2004 release of Models-3 CMAQ. Atmospheric Environment 40, 4811–4824.

Environmental Protection Agency, 2005. Evaluating ozone control programs in the eastern United States: focus on the NO_x budget trading program, EPA454-K-05-001, 〈http://www.epa.gov/airtrends/2005〉.

Frost, G.J., McKeen, S.A., Trainer, M., Ryerson, T.B., Neuman, J.A., Roberts, J.M., Swanson, A., Holloway, J.S., Sueper, D.T., Fortin, T., Parrish, D.D., Fehsenfeld, F.C., Flocke, F., Peckham, S.E., Grell, G.A., Kowal, D., Cartwright, J.,

Auerbach, N., Habermann, T., 2006. Effects of changing power plant NO_x emissions on ozone in the eastern United States: proof of concept. Journal of Geophysical Research 111, D12306.

Gego, E., Porter, P.S., Gilliland, A., Rao, S.T., 2007. Observation-based assessment of the impact of nitrogen oxide emissions reductions on ozone air quality over the eastern United States. Journal of Applied Meteorology and Climatology 46, 994–1008.

Gilliland, A.B., Hogrefe, C., Pinder, R.W., Godowitch, J.M., Rao, S.T., 2007. Dynamic evaluation of regional air quality models: assessing changes in O_3 stemming from changes in emissions and meteorology. Atmospheric Environment, in review.

Grell, G.A., Dudhia, J., Stauffer, D.R., 1994. A description of the fifth-generation Penn State/NCAR mesoscale model (MM5). NCAR Technical Note, NCAR/TN-398+STR, Boulder, CO.

Hogrefe, C., Rao, S.T., Zurbenko, I.G., Porter, P.S., 2000. Interpreting the information in ozone observations and model predictions relevant to regulatory policies in the eastern United States. Bulletin of the American Meteorological Society 91, 2083–2106.

Kim, S.W., Heckel, A., McKeen, S.A., Frost, G.J., Hsie, E.Y., Trainer, M.K., Richter, A., Burrows, J.P., Peckham, S.E., Grell, G.A., 2006. Satellite-observed US power plant NO_x emission reductions and their impact on air quality. Geophysical Research Letters 33, L22812.

Ozone Transport Assessment Group, 1997. OTAG Final Report. Available online at: 〈http://www.epa.gov/ttn/rto/otag/finalrpt〉.

Rao, S.T., Zurbenko, I.G., Neagi, R., Porter, P.S., Ku, J.Y., Henry, R.F., 1997. Space and time scales in ambient ozone data. Bulletin of the American Meteorological Society 78, 2153–2166.

Solberg, S., Bergstrom, R., Langer, J., Laurila, T., Lindskog, A., 2005. Changes in Nordic surface ozone episodes due to European emission reduction in the 1990s. Atmospheric Environment 39, 179–192.

White, A.B., Darby, L.S., Senff, C.J., King, C.W., Banta, R.M., Koermer, J., Wilczak, J.M., Neiman, P.J., Angevine, W.M., Talbot, R., 2006. Comparing the impact of meteorological variability on surface ozone during the NEAQS (2002) and ICARTT (2004) field campaigns. Journal of Geophysical Research 112, D10S14.

Xiu, A., Pleim, J.E., 2001. Development of a land surface model, part 1: applications in a mesoscale meteorology model. Journal of Applied Meteorology 40, 192–209.

Zhang, J., Rao, S.T., 1999. The role of vertical mixing in the temporal evolution of ground-level ozone concentrations. Journal of Applied Meteorology 38, 1674–1691.